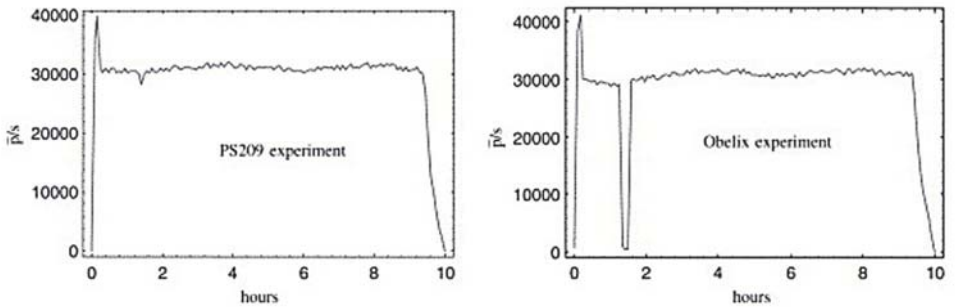

Fig. 6.11. Spill of antiprotons to two experiments. Each point on the curve is the number of particles recorded per s averaged over 10 s. The brief dip in the spill-rate of OBELIX is a pause for calibration.

6.5 The UA1 Tracker: An Electronic Bubble Chamber

Bernard Sadoulet

Physics goals and detector design philosophy

The priority for the UA experiments was the detection of the putative W and Z bosons of the Standard Model [Box 6.4] with emphasis on their "golden" signatures of their leptonic decay modes $W \rightarrow e\nu$ or $\mu\nu$ and $Z \rightarrow ee$ or $\mu\mu$, producing high transverse momentum charged leptons. Another major goal was the search for physics beyond the Standard Model, revealed by e.g. the simultaneous production of electrons and muons with specific charge configurations.

The accent was therefore put on the precise measurement of leptons, implying new performance requirements on the charged particle detector measuring the curvature of their tracks inside the magnetic field. The required excellent identification of the electrons would be obtained by comparing their momenta measured in the central tracker with their energies measured in the electromagnetic calorimeter. Muons would be identified as tracks penetrating through a metre of the iron return yoke of the magnet and by comparing the momentum measured in the central detector with that estimated from their deflection in the magnetized iron, obtained from the direction of the track emerging behind the yoke.

The measurement of high transverse momentum "jets" of particles was another design requirement of the UA1 detector. These jets could signal the emission of quarks or gluons, originating e.g. from the dominant quark–antiquark decay modes of the W and Z. Jets had been hinted at by experiments at the ISR (and later observed by AFS collaboration [Highlight 4.11], but at the ISR energy they were broad and difficult to identify. At the energy of the p–$\bar{p}$ collider, however, they were expected to be fairly easily detectable as a group of collimated particles.

Electromagnetic and hadronic calorimetry would measure their total energy, including the neutral particles (π^0's and neutrons).

The collaboration recognized rapidly that a detector was needed covering as much as possible of the solid angle around 90° from the beams. This is a prerequisite for the detection of the W or of any new physics based on "missing transverse energy", signalling the escape of a neutrino or possibly other neutral non-interacting particles such as supersymmetric particles [Box 7.2]. The design therefore aimed at achieving as close a "hermetic", i.e. 4π solid angle coverage, as possible, minimizing regions where particles could not be detected.

The geometry of the magnet was a major topic of discussion. The choice was between a solenoid coaxial with the beams or a dipole with its field perpendicular to them. While considerations of symmetry favoured a solenoid, a dipole was finally chosen. This was motivated in large part by the requirement of a detector with a fairly large aspect ratio (6 m long with a diameter of 2.5 m), in order to match the topology of the final states produced in the collisions. A solenoid would have to be instrumented with a self-supporting drift chamber with 6 m long wires, for which the technology was not available, and the CERN engineering team came forward with a very elegant solution for a tracking detector optimized for the dipole [Box 4.4]. To meet the short construction time a conventional warm magnet was adopted with a 0.7 T field and a magnetic volume of 80 m^3.

The UA1 tracker

With the spectrometer magnet chosen, the collaboration converged rapidly on the technology of the central detector. This instrument had to offer very good spatial resolution, high efficiency for reconstructing tracks in events of very high particle multiplicities and a bubble-chamber like clarity of the track pattern to clearly expose the precious leptons. The "Time Projection Chamber", invented in 1974 [32], shows this kind of performance and this concept was adapted to the UA1 magnet geometry. Instead of measuring the track curvature in projection, the measurement of the drift time was used due to its intrinsic precision; this led to having the sense wires parallel to the magnetic field. The design goal materialized in a drift chamber system with 6000 sense wires [Box 4.5]. The novel electronic read out could register several independent hits on a drift wire per collision, simultaneously digitizing the drift time and the charge information, which allowed a pictorial track reconstruction in three dimensions. At the time, this tracker (Fig. 6.12) was at the frontier of drift chamber development [Highlight 4.8].

Detecting invisible particles **Box 6.3**

Particles properties are revealed in particle detectors, devices in which the particle "interacts" and leaves a telltale signal [Box 3.2]. No single detector can measure all their properties and several specialized ones are combined in an experiment. Through electromagnetic (e-m) interaction, charged particles ionize or excite a specially chosen material in the detector. It may be a gas [Highlight 4.8], a liquid [Highlight 5.6] or a solid [Highlight 5.9]. The level of ionization or excitation depends characteristically on the particle velocity v [Box 5.2]. A variety of detectors have been developed to measure position, velocity and energy of the particles.

Tracking detectors measure the charged particle position or trajectory. They have one important and distinct feature: a very gentle interaction, hardly influencing the properties of the particle, suffices to produce a useful signal.

When these detectors are immersed in a magnetic field B, the radius of curvature ρ of the charged track, proportional to p/qB (where q is the charge), gives its *momentum* p. The figure of merit of such a "spectrometer" is its accuracy, expressed as $\Delta p/p, \approx p\ \sigma/\ B\ L^2$, where σ is the precision of the position measurement and L the distance over which the particle track is analysed. This explains the quest for improved σ and higher B, and the increasing size (L) of the spectrometers to measure ever increasing p [Highlight 8.12].

Other instruments measure the *energy* E. Interacting via e-m and/or strong interaction the particle develops a *cascade ("shower")* of particles absorbed in a massive detector. Nearly all E of the incident particle is finally transferred to excitation of the absorber molecules, increasing its temperature, whence the name "*calorimeter*". The absorber is usually instrumented with detectors sensitive to the cascade of particles [Highlight 4.10], but can also be sensitive in its full volume [Highlight 7.9]. The number of cascade particles being proportional to E, the statistical accuracy of the E measurement is $\approx 1/\ E^{1/2}$, a bonus for high E. Calorimeters work for both charged and neutral particles.

To *identify a particle* via its mass, one needs p and its velocity v. Besides time of flight measurement for slow particles [Highlight 8.9], one uses also the v dependence of e-m processes: ionization, Cherenkov or transition radiation [Highlights 4.9, 7.8]. Charm or beauty particles live of the order of 10^{-12} s. Being produced with v close to the speed of light, the relativistic time dilation lets them fly of the order of 1 mm before decaying, a decay pattern accessible to Pixel detectors [Highlight 8.6]. Assembling such specialized detectors leads to the typical onion-like sequence at colliders. "Fixed target" experiments (such as COMPASS, Chapter 5) have a quite different structure.

These detectors, first developed for particle physics, are now frequently found in medical diagnostic and imaging techniques [Highlights 10.3, 10.4].

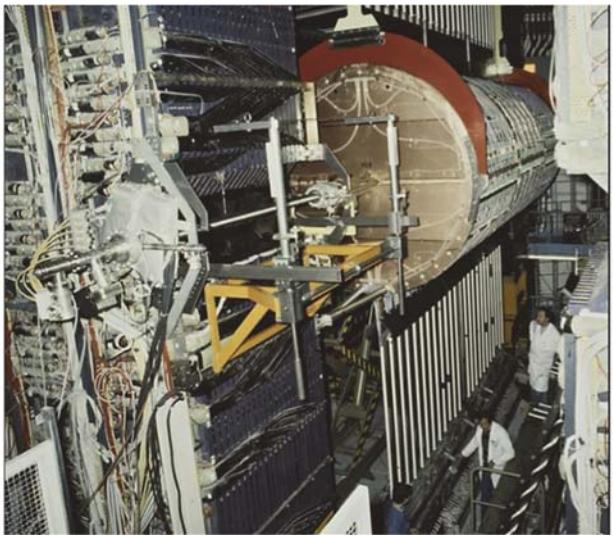

Fig. 6.12. Partial view of UA1. The detectors surrounding the long, cylindrical central tracker are retracted to provide access to the Tracker. The thin beam pipe traverses the centre of the tracker.

The mechanical design was very innovative. As a self-supporting cylinder, made of six independent half-cylinder chambers, each with a length of 2 m and a diameter of 2.2 m (Fig. 6.13a), it provided close to 4π coverage of the collision products and achieved the bubble chamber-like "view" of the events (Fig. 6.14). One striking feature of the system was the cylindrical shell of the chambers supporting the wires, made with a pre-stressed honeycomb structure, sandwiched between glass fibre-epoxy layers. The amount of applied pre-stress was calculated to precisely balance the tension applied to the wires.

The 6000 sense wires (10 mm spacing, up to 2.2 m length) and the 17 000 field-shaping wires were parallel to the magnetic field. They were organized in horizontal planes in the four forward modules, and in vertical planes in the two central ones. This arrangement is a consequence of the horizontal magnetic field. With this orientation of the wire planes approximately the same number of measurements along the tracks over the detector volume was obtained, given the expected topology of the interactions and the dipole magnetic field. A typical drift cell is shown in Fig. 6.13b. The electrostatic forces were controlled with an intermediate field plane at voltage V_c, while V_f controlled the gas amplification. The position of the sense wires in a plane was known within 50 microns, the coordinate of a "typical" plane to about 200 microns, a tribute to the engineering quality of the supporting structure.

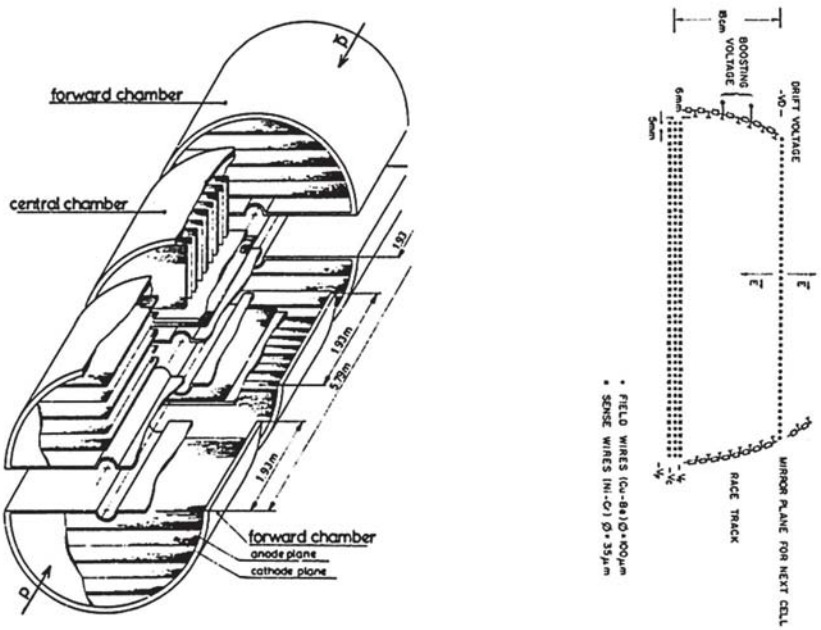

Fig. 6.13. Left: exploded view of the six half-cylinders constituting the central tracker; right: cross-section through a half-cylinder, showing the arrangement of signal wires and wire electrodes shaping the drift field and the signal amplification region.

The longest drift distance was 18 cm, such that at a 1.5 kV/cm drift field the drift time was less than the interval between bunches (3.8 μs). This drift length also limited the distortion of the electric field by space charge from backgrounds from the machine. The state-of-the-art signal processing used 6-bit "Flash Analogue-to-Digital Converters (FADCs), two per sense wire, digitizing the induced signal charge. The sense wire had kΩ level resistance; the ratio of the charges recorded at each end gave a measure of the longitudinal position of the charge along the wire to about 2% of the wire length. The drift time was measured with Time-to- Digital Converters (TDCs) with 4 ns accuracy. The digital outputs of TDCs and FADCs were stored in a buffer memory, recording the event history of the preceding 4 μs. The data volume (1.6 MB) was impressive at the time and had to be synchronously reduced by processors.

The analogue signal processing electronics required careful calibration. The linearity was calibrated by injecting a precisely known and variable charge into the preamplifiers. For each drift cell, the relevant voltages and currents were precisely measured and monitored. An alarm system provided fast indications of any malfunctioning.

To achieve the intrinsic performance of the tracker a number of parameters had to be measured and controlled, such as temperature, gas mixture variations and distortions of the electric fields. Two independent methods were used. Artificial straight tracks were generated with precisely positioned ionizing X-ray and laser beams. Secondly, the built-in "auto-calibration" of the detector was used, made possible by the special drift cell structure: as two adjacent drift spaces had opposite E-fields, tracks traversing them had to "line up" in a correctly calibrated detector. These efforts paid off. The globally achieved resolution of the drift distance was a most remarkable 290 microns for the reconstructed tracks.

Figure 6.14 shows an historical event, the first W decay recorded in the UA1 experiment. With its combination of optimal detection geometry, matching well the expected interesting collision topologies, an advanced technology for the support structures, innovations in electronics, calibration and read-out, this tracker was at the cutting edge of technology and the first true "electronic bubble chamber". Its quality and reliability were a key to the Nobel Prize-winning success of UA1.

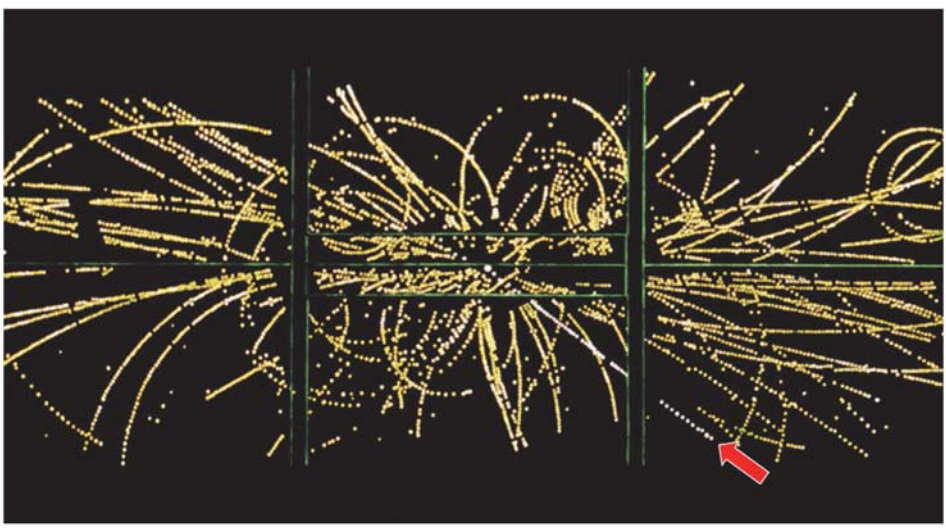

Fig. 6.14. The first observed W-decay, as recorded in the central tracker.

The Standard Model (SM) **Box 6.4**

The SM is a remarkably successful theoretical description of the elementary particles and their interactions, from which our visible world is built. It ignores gravity, described by the General Theory of Relativity. Figure 1.2 shows the SM constituents (fermions of spin 1/2). The carriers of the 3 types of forces between fermions, bosons of spin 1, are shown in Fig. 1.3. To these elementary objects, one must add the spin 0 Higgs boson.

The SM describes mathematically the particles as field quanta. These exist not only in space-time, but also "live" in abstract, so-called *internal spaces* (Fig. 1.2). E.g., a quark lives in the 3-D space of *colour*, in which it can be thought of as a vector. The subscripts L (Left) and R (Right) refer to their handedness H [Box 2.2] and point at a basic feature of the SM that the behaviour depends on H: in the *weak isospin* (WI) *space,* LH ones live in couples, RH ones as singles. In the SM the W couples only to LH fermions.

In such spaces, one can think of performing "rotations": for instance, a rotation in colour space changes a blue quark into a red quark. Or, in the WI space, an e^- rotates into a neutrino, or a strange quark into a charm quark. The SM gives the processes: emission of a gluon in the former case, of a W boson in the latter. There is thus a unique mode of interaction between fermions, whatever the force: the exchange between them of the relevant boson, as suggested by the diagrams of Fig. 1.3.

The SM provides the mathematical framework describing these rotations. But it does much more: its guiding principle posits the freedom to perform any arbitrary such rotation *locally,* i.e. in any point of space-time, without changing the physics, which cannot depend on an arbitrary choice of local coordinates. The equations of the SM must thus be invariant (symmetrical) under the relevant rotation. This symmetry requirement is a great help in defining the actual mathematical formulation. Such a rotation of the field configuration is called a "gauge" transformation (GT). The lack of change (invariance) of measurable quantities under a GT is called *gauge invariance*.

In quantum electrodynamics, QED [Box 2.3], describing e.g. the e^- and γ, the GT changes the phase of the e^- wave function, through γ emission by the e^-. The γ feels the e^- electric charge but does not carry it. Being neutral it does not self-interact (SI).

An important success of the SM is a unified description of QED and the weak interaction, the Electroweak Interaction. Its "abstract" bosons W^0, B^0 (not shown in Fig. 1.3) "mix" to give the physical γ and Z^0, through the mixing angle θ_W [Box 7.1]. The initial unified formulation (in 1961) only worked however for massless particles, and could not explain fully our perception of reality. The BEH mechanism [Box 8.2] completed the picture, enabling the SM to much better describe the visible world.

In the weak and QCD sectors, W/Z and gluons feel and carry the weak and colour charge, respectively, and *self-interact*. Gluon SI is responsible for the specific properties of the strong interaction [Box 4.2].